Real-time simulation of a guitar power amplifier

Ivan Cohen, Thomas Hélie

REAL-TIME SIMULATION OF A GUITAR POWER AMPLIFIER

Ivan Cohen

Orosys / Two Notes,
Ircam - CNRS - STMS UMR 9912,
Montpellier, France
ivan.cohen@orosys.fr

Thomas Helie

Ircam - CNRS - STMS UMR 9912,
Analysis/Synthesis Team
Paris, France
thomas.helie@ircam.fr

ABSTRACT

This paper deals with the real time simulation of a class A single ended guitar power amplifier. Power tubes and triode models are compared, based on Norman Koren's work. Beam tetrodes and pentodes characteristics are discussed, and displayed as Norman Koren's model parameters. A simple output transformer model is considered, with its parameters calculated from datasheets specifications. Then, the circuit is modeled by a nonlinear differential algebraic system, with extended state-space representations. Standard numerical schemes yield efficient and stable simulations of the stage, and are implemented as VST plug-ins.

1. INTRODUCTION

Many analog audio circuit simulations (guitar amplifiers, synthesizers, studio devices etc.) have been released for musicians, who want to replace their equipment with cheaper and more flexible digital equivalents. However, the realism of these digital simulations can still be improved. This is mainly due to nonlinearities that are responsible for the "sound signature of analog audio devices" the modeling of which is often complex and still keeps a lot of people busy.

This paper deals with realistic simulation of guitar tube amplifiers, for real-time applications. Several papers have been published about this subject, often focused on triode amplifiers circuits, and sometimes power amplifiers (see [1, 2, 3, 4, 5]). In this article, we consider a single-ended tube power amplifier, using pentodes and an output transformer. First, we consider Norman Koren's model for several standard power tubes found in guitar power amplifiers. The control grid current and the parasitic capacitances are studied, and compared with the work done in [5] about triodes. Then, a simple linear model for the output transformer is introduced, with its parameters calculated from datasheets specifications. The circuit is simulated in real time using extended state space representations. Finally, the results are shown and discussed.

2. THE CLASS A POWER AMPLIFIER

The class A power amplifier (figure 1) increases the power of the signal from a preamplifier to a speaker, with a matched output impedance. This is a very simple power amplifier, chosen for its sound characteristics, and for the simplicity of its modelisation. It is defined as "single ended" because it uses a single tube to produce an output, in contrast to push-pull amplifiers, another topology using more tubes and phase inverters for more power, operating in classes AB or B (see [6] for more information about power amplifiers classes). The voltages V_{b1} and V_{b2} are constant bias voltages. Typical values for its components can be seen in table 1.

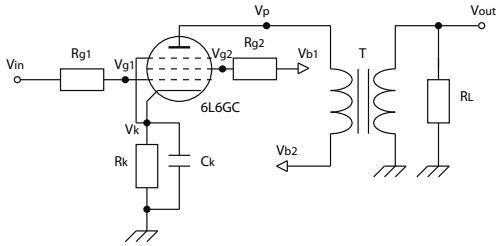

Figure 1: The electronic circuit

Vb1	Vb2	Rg1	Rg2	Rk	RL	Ck
300 V	400 V	5.6 kΩ	1 kΩ	220 Ω	8 Ω	100 μF

Table 1: Typical values of the components used in the power amplifier

The passive components are considered ideal. Using the Millman's theorem, Kirchoff laws and our component models, the electronic circuit can be modeled by a set of differential algebraic equations.

3. POWER TUBES MODELS

3.1. Introduction

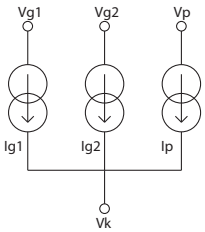

Figure 2: The power tube's model

As seen in [7, 5], the triode has a capacitive behaviour between the grid and the plate, increased by the Miller effect. The adding of the screen grid decreases the value of the capacitance (from 2 pF to 0.02 pF), and increases the power gain of the vacuum tube (μ is the voltage gain). This yields to a topology called the tetrode, which has a unwanted side-effect, known as the Dynatron effect. It gives the tetrode valve a distinctive negative resistance characteristic, sometimes called "tetrode kink". This problem has been solved with the addition of a third grid (the pentode patented by Philips/Mullard [8]), and with another topology called the beam

tetrode. These two kinds of vacuum tubes are very often described as pentodes.

The pentode is a vacuum tube widely used in guitar and hifi power amplifiers, a triode with the control grid (G1), the cathode (K), the plate (P), and two extra pins : the screen grid (G2) and the suppressor grid (G3). Beam tetrodes and pentodes plate current curves in datasheets show they have a significantly different behaviour. In short, beam tetrodes have much sharped knees compared to pentodes, a lower ratio of screen to plate current, a lower third harmonic distortion [6]. Their model is very important for the realism of the complete stage's simulation.

3.2. Norman Koren's model

The Norman Koren's model [1] is said "phenomenological". It models the behavior of physical phenomena using parameters not derived from fundamental physics, to match published curves from datasheets. The expression of the I_p and I_{g2} currents for pentode-like vacuum tubes are the following :

$$E_1 = \frac{V_{g2k}}{K_p} \log\left[1 + \exp\left(K_p\left(\frac{1}{\mu} + \frac{V_{g1k}}{V_{g2k}}\right)\right)\right] \quad (1)$$

$$I_p = \frac{E_1^{E_x}}{K_{g1}}(1 + \text{sgn}(E_1)) \arctan\left(\frac{V_{pk}}{K_{vb}}\right) \quad (2)$$

$$I_{g2} = \exp\left(E_x \log\left(\frac{V_{g2k}}{\mu} + V_{g1k}\right)\right) \quad (3)$$

The table 2 displays typical tubes parameters, from [1] and SPICE models. μ is the voltage amplification factor, K_{g1} a parameter inversely proportional to overall plate current, E_x an exponent, K_{vb} a knee parameters in volts, K_{g2} the inverse screen grid current sensitivity, and K_p a parameter that affects the plate currents for large plate voltages and large negative grid voltages. The differences between the pentodes and the beam tetrodes in general are displayed in this table, particularly with the parameters μ and K_{vb}.

Pentode	μ	K_{g1}	K_{g2}	K_p	K_{vb}	E_x
EL34	11	650	4200	60	24	1.35
EL84	16	570	4200	50	24	1.35
Beam Tetrode	μ	K_{g1}	K_{g2}	K_p	K_{vb}	E_x
6L6GC	8.7	1460	4500	48	12	1.35
KT88	8.8	730	4200	32	16	1.35

Table 2: The parameters of Norman Koren's model for a few pentodes and beam tetrodes

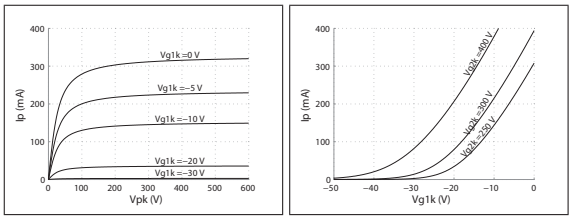

Figure 3: Norman Koren's model for the I_p current

3.3. Grid current and parasitic capacitances

The I_{g1} current is often neglected in triode models [3, 9]. But it is responsible for the grid rectification effect that designers try to limit using specific polarizations and the resistance R_{g1}. In [5], the grid current model was a simple approximation of a diode's characteristic. A smooth transition is added between the resistive behaviour and the interval of voltages where the current is null, with a second order polynomial. This model gives results close to SPICE's diode models. The parameter R_{g1k} controls the resistive behaviour of the grid current, V_γ is the voltage threshold between the null and resistive behaviour. The parameter K_n is the length of the smooth transition.

$$I_{g1} = \begin{cases} 0 & \text{if } V_{g1k} < V_\gamma - K_n \\ \frac{V_{g1k} - V_\gamma}{R_{g1k}} & \text{if } V_{g1k} > V_\gamma + K_n \\ aV_{g1k}^2 + bV_{g1k} + c & \text{otherwise} \end{cases} \quad (4)$$

with

$$\begin{aligned} a &= \frac{1}{4K_n R_{g1k}} \\ b &= \frac{K - V_\gamma}{2K_n R_{g1k}} \\ c &= -a(V_\gamma - K_n)^2 - b(V_\gamma - K_n) \end{aligned} \quad (5)$$

V_γ	R_{g1}	K_n
13 V	6000 Ω	3 V

Table 3: Typical values for the parameters of grid current's model

In [5], we consider the dynamic behaviour of the triode model with its parasitic capacitances, in particular the capacitance between the grid and the cathode, because of the Miller effect. Pentodes and tetrodes have lower parasitic capacitances than triodes. The parameter μ is lower than 20, instead of 100 for 12AX7 triodes. So, considering the Miller effect for pentode-like tubes, the capacitances have no effect inside the bandwidth of audible frequencies, and including parasitic capacitances in tube models is not judged relevant. This result has been confirmed by SPICE simulations and informal listening tests.

4. OUTPUT TRANSFORMER MODELS

Vacuum tube power amplifiers typically have a tube output impedance around 1 kΩ, whereas loudspeakers have an impedance between 4 and 16 Ω. The high-impedance plate speaker load is transformed into a low-impedance load using an output transformer. The ideal output transformer is defined by the number of turns in its primary winding N_p and in its secondary winding N_s. The ratio between the input and output impedance of the transformer is a function of $(N_p/N_s)^2$.

We consider the Plitron PAT-3050-SE-02 output transformer, a typical output transformer for single ended power amplifiers. The relevant information for our model is available on Plitron datasheets, and in the table 4.

4.1. A simplified model

The transformer's model has been developed by Plitron and adapted by Norman Koren [1]. Its schematic is displayed in the figure

Total primary inductance	L_p	40 H
Primary leakage inductance	L_{sp}	10 mH
Quality factor = L_p/L_{sp}	Q	4000
Turns ratio	$N = N_p/N_s$	35.551
Total primary resistance	R_{ip}	80 Ω
Total secondary resistance	R_{is}	0.1 Ω

Table 4: Information about the Plitron PAT-3050-SE-02 output transformer

4, and its parameters are calculated according to the datasheet in the table 5.

$$\begin{aligned} L_2 &= L_p/N^2 \\ M_{12} &= \sqrt{1-1/Q}\sqrt{L_1 L_2} \end{aligned}$$

R_{in}	R_{out}	L_1	L_2	M_{12}
80 Ω	0.1 Ω	40 H	0.0316505 H	1.125035 H

Table 5: The parameters of the output transformer's model used in simulation

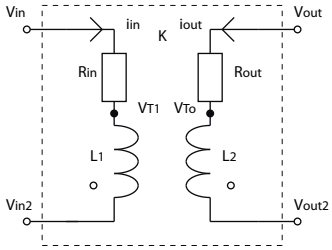

Figure 4: Simplified output transformer model

5. NUMERICAL SCHEMES

5.1. Extended State-Space Representations

5.1.1. Presentation

Linear state-space representations are well known in control engineering. For nonlinear cases, nonlinear functions can be introduced in their classical formulation. Moreover, the nonlinearity can introduce implicit equations. We have suggested an extended state-space representation in [5], to separate the differential equations of implicit problems, with the introduction of a static nonlinear vector W. This is a similar but more general state-space representation for nonlinear systems than the K-method (see [10]). Let X be the dynamic state vector of the studied system, W a static nonlinear state, U the input vector and Y the output vector.

$$dX/dt = f(X,W,U) \quad (6)$$

$$0 = g(X,W,U) \quad (7)$$

$$Y = h(X,W,U) \quad (8)$$

Remark : the linear case is a particular extended state space representation without the function g, with dim $W = 0$ and the functions $f(X,U) = AX + BU$ and $h(X,U) = CX + DU$ (A, B, C and D are constant matrices).

5.1.2. Circuit Equations

The dynamic behavior of the circuit is caused by the capacitors and inductances. The nonlinearity comes from the tube modeling, the expression of the currents I_p, I_{g1} and I_{g2}. Let the state variables be :

$$\begin{aligned} U &= V_{in} \\ X &= [V_k \quad V_{T1} - V_p \quad V_{out} - V_{TO}]^T \\ W &= [V_{g1} \quad V_{g2} \quad V_p]^T \\ Y &= V_{out} \end{aligned}$$

The dimension of the vectors X and W are both equal to three. The state space representation of the class A power amplifier stage is the following :

$$f = \begin{cases} \left[I_{g1} + I_{g2} + I_p - \frac{X_1}{R_k}\right] \frac{1}{C_k} \\ \frac{D}{\Delta}\left[V_{b2} - X_2 - W_3\right] - \frac{B}{\Delta}\left[\frac{R_L}{R_{out}} - 1\right] X_3 \\ \frac{A}{\Delta}\left[\frac{R_L}{R_{out}} - 1\right] X_3 - \frac{C}{\Delta}\left[V_{b2} - X_2 - W_3\right] \end{cases} \quad (9)$$

$$g = \begin{cases} W_1 - U + R_{g1} I_{g1} \\ W_2 - V_{b1} + R_{g2} I_{g2} \\ -X_2 + R_{in} I_p \end{cases} \quad (10)$$

$$h = \frac{R_L}{R_{out}} X_3 \quad (11)$$

with

$$\begin{aligned} A &= \frac{L_1}{R_{in}}, B = \frac{M_{12}}{R_{out}}, C = \frac{M_{12}}{R_{in}}, D = \frac{L_2}{R_{out}} \\ \Delta &= AD - BC \end{aligned}$$

The currents are functions of X, W and U. This extended state space representation yields to a numerical simulation with standard methods of resolution, for differential and implicit equations.

5.2. Discretization

Discretization of the extended state-space equations is done with the resolution of differential and implicit equations. Their complexity is a consequence of the numerical scheme chosen for the resolution, and the existence of nonlinear delay-free loops in the electronic circuit. T_e is the sampling period.

5.2.1. Differential equations

To solve the ordinary differential equations (equation 6), explicit Runge-Kutta methods are often used [11, 12]. Implicit methods are also used to solve stiff problems (see [5]), as the trapezoidal method (equation 12), often called bilinear transform and widely used in digital signal processing [13].

$$\begin{aligned} X_{n+1} &= X_n + \frac{T_e}{2} f(X_{n+1}, W_{n+1}, U_{n+1}) \\ &\quad + \frac{T_e}{2} f(X_n, W_n, U_n) \end{aligned} \quad (12)$$

We have seen in [5] that the consideration of the parasitic capacitance C_{gp} in the model makes a stiffness problem appear, and requires the use of implicit numerical schemes. Stiffness can be considered as a differential equation with some terms that can lead to rapid variation in the solution. In equations 9, the coefficient Δ is around 10^{-6}. The use of implicit algorithms is necessary to guarantee the stability.

5.2.2. Implicit equations

The standard method of Newton-Raphson is used to solve implicit equations written $f(Z) = 0$ with Z a vector of any dimension, and find its roots. This method solves equation 7, but also equation 6 if implicit methods of differential equation's resolution are used. So, Z is the vector $[X \quad W]^T$.

Let Z_n^k be the approximative value of Z at the iteration k of the algorithm for the sample n. $J_f(Z)$ is the Jacobian matrix of $f(Z)$.

$$Z_n^{k+1} = Z_n^k - J_f^{-1}(Z_n^k) \times f(Z_n^k) \tag{13}$$

This algorithm converges to a solution if the derivatives are Lipschitz continuous and locally isomorphic around the solution [11, 12]. This is the case if the initial value Z_n^0 is close enough to the solution. Our numerical scheme works well, with 4 iterations, if we choose the previous state Z_{n-1} as the initial value, with high sampling frequencies (typically in megahertz), to ensure that successive samples are close in value to each other.

6. DISCUSSION

The main purpose of power tube stages is to increase the power of the signal. Input voltages are around a few volts in general : the stage adds a few harmonics to the signal's content, with an impact on the sound which is less important than what is done by preamplifiers stages. If the input voltage is higher, distortion appears from the power tubes and the output transformers. This phenomenon occurs typically in "vintage" guitar amps.

In our simulation, the nonlinear behaviour of the transformer is not considered. A sinousoid with a frequency of 2000 Hz and an amplitude of 30 V feeds the input of the simulated stage, with a 6L6GC beam tetrode. The output is displayed in the figure 5.

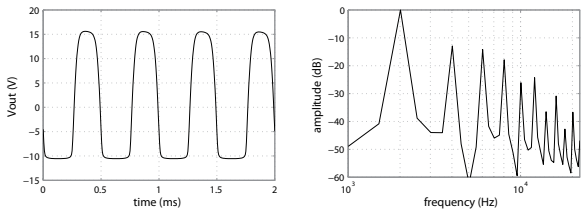

Figure 5: Output signal and harmonic response for an input sinusoid (2000 Hz 30 V)

The output does not change significantly when we replace the tube models. The only perceptive phenomenon is the gain difference between tubes with this model. More differences may be listenable if a more complex circuit had been modeled, with coupling between the circuit and a speaker. Sound samples are available on `http://www.orosys.fr/cohen/samples.htm`.

7. CONCLUSION

This study has shown a way to simulate a simple class A power amplifier, using extended state-space representations, the tube model of Norman Koren, and a linear model of the output transformer. It yields to the implementation of plug-ins, which produces satisfactory sounds with standard cabinet simulations. Moreover, future work will be dedicated to model and simulate other topologies of guitar power amplifiers, phenomenon such as feedback and sag, the coupling between each element of a guitar amplifier, and the nonlinearities of output transformers, such as hysteresis effects.

8. REFERENCES

[1] Norman Koren, "Improved vacuum tube models for spice simulations," *Glass Audio*, vol. 5, no. 2, pp. 18–27, 1996.

[2] David T. Yeh and Jyri Pakarinen, "A review of digital techniques for modeling vacuum-tube guitar amplifiers," *Computer Music Journal Summer 2009*, vol. 33, no. 2, 2009.

[3] Jyri Pakarinen and Matti Karjalainen, "Wave digital simulation of a vacuum-tube amplifier," in *IEEE International Conference on Acoustics, Speech and Signal Processing*, 2006.

[4] Jyri Pakarinen Miikka Tikander and Matti Karjalainen, "Wave digital modeling of the output chain of a vacuum-tube amplifier," in *12th Int. Conference on Digital Audio Effects (DAFx-09)*, Como, Italy, 2009.

[5] Thomas Helie and Ivan Cohen, "Simulation of a guitar amplifier stage for several triode models : examination of some relevant phenomena and choice of adapted numerical schemes," in *127th Convention of the Audio Engineering Society*, New York, USA, 2009.

[6] Richard Kuehnel, *Vacuum Tube Circuit, Design Guitar Amplifier Power Amps*, Pentode Press, 2008.

[7] Morgan Jones, *Valve Amplifiers*, Newnes, third edition, 2003.

[8] W.L. Krahl, "Pentode tube," US Patent 1869568, 1932.

[9] David T. Yeh and Julius O. Smith III, "Simulating guitar distortion circuits using wave digital and nonlinear state-space formulations," in *11th Int. Conference on Digital Audio Effects (DAFx-08)*, Espoo, Finland, 2008.

[10] Giovanni De Poli, Gianpaolo Borin, and Davide Rocchesso, "Elimination of delay-free loops in discrete-time, models of nonlinear acoustic systems," *IEEE Transactions on Speech and Audio Processing*, vol. 8, no. 5, pp. 597–605, September 2000.

[11] Jean-Pierre Demailly, *Analyse numérique et équations différentielles*, Collection Grenoble Sciences, 2006.

[12] J. Stoer and R. Bulirsch, *Introduction to Numerical Analyisis*, Springer New York, third edition, 2002.

[13] David T. Yeh et al., "Numerical methods for simulation of guitar distortion circuits," *Computer Music Journal*, vol. 32, no. 2, 2008.

[14] Linear Technology, "LTSpice IV," Available at http://www.linear.com/, 2010.